Proton Exit Channels in Bovine Cytochrome c Oxidase

ARTICLE *in* THE JOURNAL OF PHYSICAL CHEMISTRY B · MARCH 2005

Impact Factor: 3.3 · DOI: 10.1021/jp0464371 · Source: PubMed

2 AUTHORS, INCLUDING:

Dragan M Popović
University of Belgrade
28 PUBLICATIONS **683** CITATIONS

SEE PROFILE

Proton Exit Channels in Bovine Cytochrome *c* Oxidase

Dragan M. Popović and Alexei A. Stuchebrukhov*

Department of Chemistry, University of California, One Shields Avenue, Davis, California 95616

Received: August 7, 2004; In Final Form: November 19, 2004

Cytochrome *c* oxidase (C*c*O) is the terminal transmembrane enzyme of the respiratory electron transport chain in aerobic cells. It catalyzes the reduction of oxygen to water and utilizes the free energy of the reduction reaction for proton pumping, a process which results in a membrane electrochemical proton gradient. Although the structure of the enzyme has been solved for several organisms, the molecular mechanism of proton pumping and proton exit pathways remain unknown. In our previous work (Popovic, D. M.; Stuchebrukhov, A. A. *J. Am. Chem. Soc.* **2004**, *126*, 1858. Popovic, D. M.; Stuchebrukhov, A. A. *FEBS Lett.* **2004**, *566*, 126), the continuum electrostatic calculations were employed to evaluate the electrostatic potential, energies, and protonation state of bovine cytochrome *c* oxidase for different redox states of the enzyme. A possible mechanism of oxygen reduction and proton pumping via His291 was proposed. In this paper, using electrostatic calculations, we examine the proton exit pathways in the enzyme. By monitoring the changes of the protonation states, proton affinities, and energies of electrostatic interactions between the titratable groups in different redox states of C*c*O, we identified the clusters of strongly interacting residues. Using these data, we detected four possible proton exit points on the periplasmic side of the membrane (Lys171B/Asp173B, His24B/Asp25B, Asp51, and Asp300). We then were able to trace the proton exit pathways and to evaluate the energy profiles along the paths. On the basis of energetic considerations and the conservation of the residues in a protein sequence, the most likely exit pathway is one via the Lys171B/Asp173B site. The obtained results are fully consistent with our His291 model of proton pumping, and provide a rationale for the absence of proton leaking in C*c*O between the pumping strokes.

1. Introduction

Cytochrome *c* oxidase is one of the key enzymes of energy transduction machinery in mitochondria and aerobic bacteria.[3−8] As the terminal enzyme of the cell respiratory chain, C*c*O[1] catalyzes the reduction of O_2 to H_2O. This reaction is coupled to proton pumping across the inner mitochondrial membrane and generation of the electrochemical proton gradient.[4,5,9] The energy stored by the proton gradient is subsequently used for ATP synthesis.[10] The key point in understanding the functional mechanism and proton pumping in cytochrome oxidase is to explain how the enzyme electron and proton transfer reactions are coupled, and to identify which residues are involved in that process. For each electron coming from the cytosolic side of the membrane and delivered by cytochrome *c*, two protons are moved across the membrane from the matrix side. One is used in chemical transformations (chemical proton), and the other is pumped across the membrane (pump proton). Two internal channels, D and K, formed by the helices of subunit A provide protons for the pumping and the chemical reaction in the active site (for the structure of C*c*O see Figure 1). The two channels are filled with water molecules which mediate proton translocation along the channels.[4] Depending on the step in the cycle, the protons can be delivered by either the K- or D-channel.[11−14] An electron transfer into the binuclear center is always accompanied by the net uptake of one proton by the enzyme for charge compensation,[15] obeying the principle of electroneutrality.[16]

Although the structure of C*c*O has been solved for several organisms, the molecular mechanism of the pumping remains unknown. While the proton entrance D- and K-channels have been identified,[17−19] the proton exit pathways remain unknown as well. A structural inspection reveals a large hydrophilic region on the exit side of the enzyme at the interface between subunits A and B containing numerous charged and polar residues and many water molecules.[18,19] Presumably, this domain is protonically well connected to the external solvent. The hydrophilicity of the proton exit channels might be a general feature of all proton pump proteins.[3] Previous studies indicated a possibility that the Mg center might be part of the water exit channel[13,20] and/or involved in a proton exit pathway.[3,21] A systematic mutagenesis study was employed on Arg438 and Arg439, pointing to their significant influence on proton translocation and indicating maybe the beginning of the proton exit channel.[22] Yoshikawa[23] proposed Asp51, on the basis of conformational changes of its side chain in different redox states, as a proton release group that is a part of a proton exit pathway. There are also controversial data about the role of the Asp364 residue, which is hydrogen-bonded to propionate A of heme a_3. In some studies, the role of this highly conserved residue among the heme−copper oxidases has been shown to be crucial for proton translocation and catalytic activity,[24−26] whereas in the other studies it has not shown any significant effect.[27,28]

This study is a continuation of our previous study[1] where electrostatic calculations were employed to investigate the

* To whom correspondence should be addressed. Fax: (530) 752-8995. E-mail: stuchebr@chem.ucdavis.edu.

[1] Abbreviations: C*c*O, cytochrome *c* oxidase; Cu_B, copper B metal center; ET, electron transfer; PLS, proton loading site; PRA, heme propionate A; PRD, heme propionate D; PRAa_3, propionate A of heme a_3; PRDa_3, propionate D of heme a_3. Our residue numbering refers to subunit A of the bovine C*c*O. If an amino acid belongs to subunit B, it is explicitly denoted.

10.1021/jp0464371 CCC: $30.25
Published on Web 01/14/2005

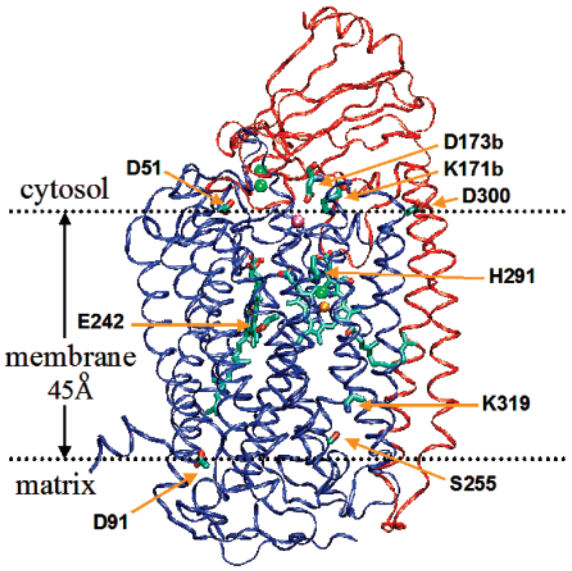

Figure 1. Structure of the molecular system of cytochrome *c* oxidase from bovine heart[23] considered in the present calculations. The core catalytic subunits A and B of cytochrome *c* oxidase are displayed as blue and red ribbons, respectively. The two hemes, *a* and a_3 (the left and right ones in the figure, respectively), and the Cu_B center (shown as a single green sphere) are located in the helical part of subunit A that is embedded in a membrane of 45 Å thickness, while the Cu_A center consisting of two copper atoms is located in subunit B, at the interface between the two subunits. The key residues along the proton-conducting channels are highlighted. The chemical and pump protons are provided from the matrix side and translocated via the entrance D- and K-channels (named after D91 and K319 residues) to the catalytic site and, according to refs 1 and 2, to the proton loading group (His291). The possible exit residues are shown on the cytosolic side of the membrane. Little is known about the proton exit path(s) taken by pump protons after leaving the active site. The main proton exit pathway elucidated from this study leads from His291 to the Asp173B/Lys171B group that is in the vicinity of the Mg center (shown as a pink sphere).

dependence of the protonation state of C*c*O (from bovine heart[23]) on its redox state and energetics of different transitions in C*c*O. On the basis of electrostatic calculations, a possible model of redox-linked proton pumping was proposed and the catalytic cycle of the enzyme was discussed.[2] The model involves His291—one of the ligands of the Cu_B redox center—as the proton loading site of the pump.[1] The pumping mechanism is based on the ET between the two hemes of the enzyme that is coupled to a transfer of *two* protons. An essential part of the pumping mechanism is kinetic gating, according to which upon the ET the transfer of a proton from Glu242 to the proton loading site His291 occurs first (fast reaction), and the transfer of the second "chemical" proton to the binuclear center (slow reaction) occurs later. The second transfer is accompanied by the ejection of the first proton from His291. The structural basis of the kinetic gating has been discussed in our previous papers.[1,2] Our recent ab initio calculations of pK_a values of the enzyme key residues[29,30] support the proposed model.

In this study, we applied the continuum electrostatic computations to address the question about the exit channels of the proton on the output side of the membrane and find specific residues responsible for proton release by the enzyme. We identified the clusters of electrostatically strongly coupled residues in a domain above the heme propionates and detected four sites (Lys171B/Asp173B, His24B/Asp25B, Asp51, and Asp300) which are the potential exit points for the pumped protons. Using the strength of electrostatic interactions between the titratable groups, important residues along the exit channels were identified.

The electrostatic component of the free energy is then calculated for different protonation microstates involving the residues of the proton exit channels. Assuming a one-dimensional model for the proton exit channel, i.e., that the proton transfer is only allowed between the adjacent protonatable sites, we were able to evaluate the energetics of proton transport along the proton exit channels. The energy profiles for the proton translocation along the three most favorable exit channels were explored and compared, suggesting that the main exit channel leads most likely to the Lys171B site. We argue that it is the energetics of proton translocation along the channels, and redox-dependent affinity switches,[31] that explains the unidirectionality of proton translocation along the channels, rather than conformational changes usually assumed in the pumping models.[21]

The proposed model is based on our theoretical prediction that His291 is the proton loading site of the pump.[1,2] In several earlier studies the possible involvement of His ligands to Cu_B was also addressed, see, e.g., refs 21, 26, and 32−34; however, no definitive conclusions could be made. The proton exit model proposed in this study is strongly linked to the His291 site and therefore provides additional ways for experimental testing of the pumping model described in refs 1 and 2.

The structure of the paper is as follows. In the next section we briefly summarize the method of calculations. In section 3, we describe the found proton exit channels. Section 4 discusses how the directionality of the proton translocation in C*c*O may be achieved, in light of the energy profiles for proton transport along the proton-conducting channels; in this section, we summarize the results of the paper.

2. Method

For the analysis of the behavior of titratable groups in the wild type of C*c*O, the continuum electrostatic calculations were employed as described in ref 1. In the calculations, the X-ray atomic coordinates and the corresponding partial atomic charges, which are placed in a low dielectric medium, describe the protein. The surrounding solvent is defined as a continuum of high dielectric constant. The mobile ions were not included in the computation, because their influence on the pumping mechanism and catalytic function of C*c*O was found to be minor.[1] Similar weak dependence on the ionic strength has been recently reported for another membrane proton pump—*bacteriorhodopsin*.[31,35−37]

The membrane was modeled as a low dielectric slab of 45 Å. The electrostatic potential of the protein−membrane−solvent system was obtained numerically on the grid by solving the Poisson equation[36,38] with the finite-difference method.[39,40] The titration curves of the protonatable groups of C*c*O were subsequently obtained by applying the Monte Carlo method.[41] For a detailed description of the method, the computational models, and the employed modifications, we refer the reader to our previous paper.[1]

In this study, the so-called model II (see our previous paper[1]), which includes the OH^-/H_2O ligand to Cu_B complex, was employed. We considered all possible redox states of the enzyme; here, however, we describe the results referring only to OORR and OORO states of the Cu_A−heme *a*−heme a_3−Cu_B redox centers of the enzyme, where O = oxidized and R = reduced state. "RR" designates the two-electron-reduced state of the binuclear complex consisting of heme a_3 and Cu_B centers, while "RO" is a state in which one metal center is formally reduced and the other is formally oxidized or, equivalently, a

state in which one of the ligands (OH^- or $=O^{2-}$) to the metal centers in the binuclear center (BNC) receives an additional chemical proton. We find that energetically the most favorable sequence of steps is one where first an electron is transferred from heme *a* to the binuclear center, converting the RO state to RR. This process is followed by a proton transfer to His291—the proton loading site (PLS) of the pump. In turn this is followed by the second proton transfer to the BNC, forming a water molecule. The entrance of the chemical proton to the BNC converts the RR state back to RO, and serves as a trigger that initiates the ejection of the preloaded pump proton from His291. Below, we consider in detail only those two redox states, RR and RO, which correspond to proton loading and proton pumping stages of the pumping cycle.

In the calculations, we first compare the proton affinities of the titratable groups in different redox states of the enzyme, and find those which change its value by more than 50 meV. Using the matrix of electrostatic couplings between the titratable groups, we then find the groups which are strongly coupled with the identified sites (i.e., those which undertake the affinity changes). The term "strong coupling" is used here for the pairwise electrostatic interactions between titratable residues of at least 100 meV, which is similar to 2 pK_a units used by Lacanster et al.[42] and Kannt et al.[43,44] From this extended set of redox-coupled residues, the possible exit pathways are selected.

There are only four groups found on the protein−solvent surface that belong to the extended set of redox-coupled residues; these are possible exit points of the pumped proton. On the other hand, we know that the pumped proton initially resides on the Nδ1 atom of His291. By shifting the proton from His291 to one of the propionates of heme a_3 (the only two available protonatable sites in direct contact with the PLS), we detect changes in the protonation affinity of the titratable sites on the surface of the protein, and narrow the possible set of exit sites on the surface of the protein. The possible exit pathways are then further examined by calculating the energies of possible intermediate protonation states and their proton connectivity. When it was necessary, we visualized the actual structure to check the hydrogen bond connectivity between the chosen sites and to assess a possibility for direct proton transfer between the two sites. In this procedure several putative exit pathways are identified; further selection is done on the basis of energetics along the putative pathways.

For the energetics calculations, we focus only on a subset of residues that make up each of the potential exit paths. In the first exit pathway we consider OH^-/H_2O in the BNC, His291, PRAa_3, Asp364, Asp173B, and Lys171B, in the second pathway OH^-/H_2O in the BNC, His291, PRAa_3, Asp364, His24B, and Asp25B, in third pathway OH^-/H_2O in the BNC, His291, PRDa_3, Arg438, Arg439, and Asp51, and in the fourth pathway OH^-/H_2O in the BNC, His291, PRAa_3, Asp364, His233, Arg302, Tyr304, Asp88B, Asp298, and Asp300.

All other titratable sites are treated as fixed in their equilibrium protonation state corresponding to a given redox state of the protein. In addition to those groups identified above, for each exit path several other potentially important residues were considered initially, such as, for instance, Tyr129 and Arg438 (in the first path), Tyr372, Tyr379, His429, and His22B (in the second path), and PRAa, PRDa, Tyr440, and His204B (in the third path), among others. We found, however, that to be considered as part of the proton transfer path all such residues, in a broad pH range around 7, require too much energy to change their corresponding protonation states, which results in energetically very unfavorable microstates.

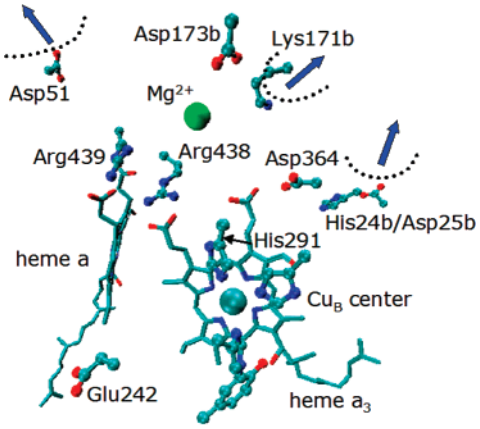

Figure 2. Relative position of the exit residues in the structure of cytochrome *c* oxidase from bovine heart.[23] The potential proton release groups in mitochondrial C*c*O—Asp51, Lys171B/Asp173B, His24B/Asp25B, and Asp300 (not shown)—are identified on the basis of the electrostatic calculations.

The main technical advancement of this study is that in addition to standard equilibrium properties we explore the nonequilibrium protonation microstates of all key titratable groups along the proton exit channels and evaluate the relative free energies of those microstates. The energetics of those microstates depends on the redox and protonation states of the enzyme. Our previous studies[1,2] have shown that the entrance of a chemical proton into the binuclear center is the key event that drives the ejection of a pump proton from the loading site, and from the enzyme. Thus, the energetics of proton translocation along the proton-conducting channels depends on the position of the chemical proton. Similar to a recent study,[31] we do not deal with the usual concept of individual pK_a values of titratable sites, but rather calculate the energy of the collective states involving all relevant protonatable sites which may take part in proton transfer from the PLS to the exit point.

To trace the proton transport along the potential exit pathways and to obtain the energetics for that process, we employed the continuum electrostatic method, which examines the nonequilibrium protonation microstates of selected collective sites. The protonation state of all other titratable groups and the redox state of the metal centers were kept fixed, and for different combinations of the microstates the energy was calculated. Energy levels were compared and the sequence of proton transfer steps was assumed on the basis of the proton transfer between the adjacent sites.

Our computational model describes a nonequilibrium proton translocation along the one-dimensional chain of protonatable sites, which make up the proton exit pathway. The main computational tool employed in this study is the free energy evaluation of proton transfer reactions between different protonatable groups of the enzyme, using the method described in detail in our previous paper.[1]

3. Exit Channels

On the basis of macroscopic electrostatic calculations, four potential proton exit sites have been identified: Lys171B/Asp173B, His24B/Asp25B, Asp51, and Asp300. They are all located on the interface among protein, membrane, and solvent in the region above the hemes, which is known to contain numerous polar and charged residues and water molecules; see Figure 1. Figure 2 shows the position of these sites relative to

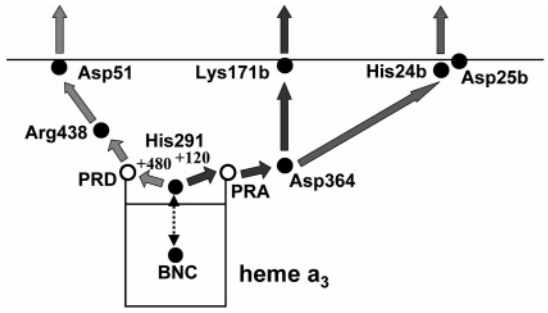

Figure 3. Schematics of the most probable proton exit pathways in the bovine C*c*O (see also Figure 1 for the structural arrangements of the key residues). The full or empty circles denote protonated or deprotonated sites, respectively. The proton population that is shown corresponds to the protonation state of the enzyme after the chemical proton has entered into the BNC.

those of the metal centers of the enzyme—Mg^{2+}, heme *a*, heme a_3, and Cu_B.

According to the model of refs 1 and 2, the pump proton resides on Nδ1 His291—one of the ligands of the Cu_B center. After the entrance of a chemical proton to the BNC, the pump proton is expelled from the Nδ1 His291 site. There are two exit routes from the His291 site—via propionate A of heme a_3, PRAa_3, and via propionate D, PRDa_3. Correspondingly, there are two exit channels. One leads to the Asp173B/Lys171B pair, coupled residues His24B/Asp25B, and Asp300 via PRAa_3, and another leads to Asp51 via PRDa_3.

The schematic of the putative proton exit channels is shown in Figure 3. The figure shows the arrangement of protons on the key amino acid residues (full circle, protonated site; empty circle, deprotonated site). The state in which both the pump proton and the chemical proton are present is metastable, because of significant proton repulsion. The state is stabilized by the ejection of the pump proton from the His291 site (PLS), gaining 260 meV in energy. However, to push a proton from His291 to the positive side of the membrane (upper side), a potential barrier must be overcome. The His291 site is hidden from the other residues, and the only contact with the "outside" is via one water molecule and the two propionates of heme a_3; see Figure 1 of ref 2 for structural details. On the other hand, PRAa_3 is hydrogen bonded to protonated Asp364, while PRDa_3 is salt bridged to the positively charged Arg438. Therefore, moving a proton from His291 in both directions (PRD and PRA of heme a_3) requires energy: +120 meV to PRA and +480 meV to PRD. Thus, in both cases the pump proton has to overcome an energy barrier to leave the metastable state on the Nδ1 site of His291.

For the exit via PRAa_3, there are three possibilities for proton release: via the Lys171B/Asp173B, His24B/Asp25B, or Asp300 site. These groups were identified as those that change their protonation state (or affinity) when a proton on Nδ1 of His291 is shifted to PRAa_3. Upon proton transfer from His291 to the PRAa_3 site, the corresponding protonation changes of the three potential exit groups, Lys171B/Asp173B, His24B/Asp25B, and Asp300, are 0.6, 0.3, and 0.1, respectively. Of the three sites Asp300 is less responsive to His291 → PRAa_3 proton transfer, because of a relatively large distance from the PRAa_3 group. The protonation change for this site is only $0.1H^+$, while the average protonation of this group is about $0.35H^+$. For this reason we excluded Asp300 from further detailed consideration, and treated it as a possible but unlikely exit site.

The exit pathway via PRDa_3 leads to the Asp51 site. The possible involvement of this residue in C*c*O proton pumping

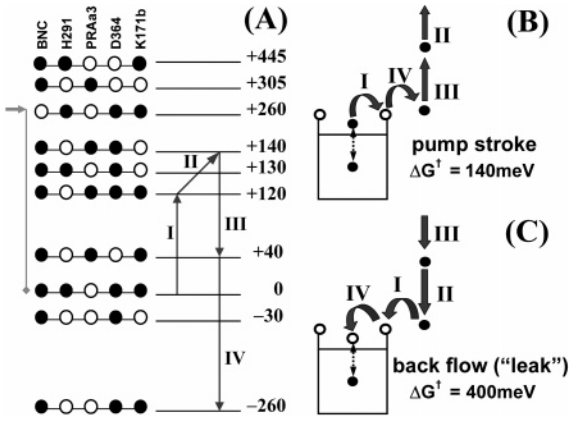

Figure 4. Lys171B proton exit pathway. (A) Energy diagram of the different protonation states of the key residues in the RO state (after the entrance of a chemical proton) of the binuclear center. Only the lowest energy levels are shown. The red arrow marks the energy level of the state (RR) before the entrance of the chemical proton into the active site. (B) Sequence of proton transfer steps in the pump stroke. (C) Sequence of proton transfer steps leading to the back-flow (leaking). The energy barriers ($\Delta G^{\ddagger}$) for both processes are evaluated.

was recently proposed by Yoshikawa and co-workers.[23,45] A cooperative model for proton pumping, involving the Asp51 residue and related to the redox-Bohr effects linked to heme *a* and Cu_A centers, was also recently discussed.[46] The detailed energy profiles along the two exit channels shown in Figure 3 are discussed next.

Lys171B Exit Pathway. In Figure 4 the energy diagram for different proton populations of the key residues along the Lys171B pathway is shown. This proton exit pathway begins with the His291 proton loading site, and involves PRAa_3, Asp364, and Lys171B residues. In addition, we find that Asp173B is very strongly coupled to Lys171B (the energy of the electrostatic coupling between their charged states is 210 meV) and there is a proton transfer pathway that connects PRAa_3, Asp364, and Asp173B. The coupling between these two residues is such that if, for example, the protonated Lys171B is mutated to a neutral residue, the unprotonated Asp173B gets protonated and therefore may work as a substitute for Lys171B. Therefore, these two residues should be considered as one proton exit site.

In the figure, only the 10 lowest energy states are shown. The red arrow marks the energy level of the state before the entrance of the chemical proton into the active site in the BNC. Transferring the proton from Glu242 to the OH^- group in the BNC leads to the formation of a water molecule and a release of 260 meV of energy. A significant driving force, despite the presence of the proton on a nearby His291, is due to the formation of a water molecule in the BNC—which is the main source of energy in the process. After the transfer of the chemical proton, the state with a proton on the His291 site becomes metastable, due to the repulsive forces between the protons on the BNC and PLS. On the basis of the energy diagram shown in Figure 4A, the first step in the ejection of the proton from Nδ1 His291 is the proton shift from Nδ1 His291 to the PRAa_3 group, which is energetically uphill by 120 meV. In the second step, Lys171B is deprotonated with the reaction free energy of +20 meV. Together with the first step, the total energy barrier for a "pump stroke" is 140 meV. The next step is proton transfer between Asp364 and Lys171B, which will reprotonate the Lys171B site, and in the last step the proton jumps from PRAa_3 to Asp364. (Proton transfer between PRAa_3/Asp364 and Lys171B may involve the water cluster around the

Mg center[47] and the Asp173B residue in a transient step or alternatively go via the backbone carbonyl groups of Asp364 and Ile365.) The last two steps, which are downhill in energy by 400 meV, form a stable state in the sense that to proceed further in the catalytic cycle an input of an additional electron to the binuclear center is required; see ref 2.

The pump stroke may also start with the deprotonation of Lys171B (130 meV, not shown), followed by the proton jump from His291 to PRAa_3 (now only 10 meV), a process that once again gives an energy barrier of 140 meV. The next two steps are identical to the previous scheme, and both are downhill in energy (total of 400 meV).

Figure 4C explains why back-flow of protons to the binuclear center and reprotonation of His291 from the output side of the membrane are kinetically hindered, which is important to prevent the leaking of protons from the periplasmic side of the membrane. The sequence of steps which leads to protonation of His291 from the periplasmic side is shown in Figure 4C. This process is the reverse of the sequence of steps of the pumping stroke shown in Figure 4B. The first step is proton jump from Asp364 to PRAa_3 that is 300 meV uphill, and the second step is proton transfer from Lys171B to Asp364 that is an additional 100 meV uphill in energy. Even if a proton from Lys171B is directly transferred to PRAa_3, which would immediately lead to state II in Figure 4, the same energy barrier remains. The total energy barrier for the back-flow is about 400 meV, which hinders the proton transfer from the periplasmic side of the membrane. The key feature of the exit channel that results in this useful property is that the last two steps of the direct transfer (pump stroke, Figure 4A) are downhill in energy with a significant driving force of 400 meV. This downhill energy in the pump stroke is the barrier for the back-flow of protons from the periplasmic side of the membrane. Thus, the protonated Asp364 residue, which is a highly conserved amino acid in all cytochrome oxidases, might be one of the key residues[24−26] which prevents the proton back-flow into the pump. The importance of the hydrogen bond between Asp364 and PRAa_3, where the proton resides on the Asp364 site, also becomes obvious.

His24B/Asp25B Exit Pathway. In the PRAa_3 exit route, after the first proton jumps from His291 to PRAa_3 (120 meV uphill transition), the two protons on the PRAa_3 and Asp364 sites will exert a repulsive "pressure" on the electrostatically coupled protonatable sites, including those on the surface of the enzyme. This repulsion will decrease their proton affinities and may result in their deprotonation. We found that, besides the Lys171B residue, the pair His24B/Asp25B particularly strongly responds to a proton transfer from His291 to PRAa_3. (The distance between Asp364 and Lys171B is 7.3 Å, while the distance between Asp364 and His24B is 11.0 Å.) The calculated deprotonation energy of the His24B/Asp25B site in this step (after the first step of proton jump to PRAa_3) is about +40 meV, which makes the total barrier 160 meV for the proton release via this group. Initially, the His24B residue is neutral with a proton on the distal Nδ1 atom that is oriented toward Asp25B and located on the solvent-exposed surface, with no proton on the proximal Nϵ1 side present. The Asp25B site is mostly (about 80%) protonated. A proton from the Asp364 side can be transferred via the chain of inner water molecules, protonating the proximal Nϵ2 position of His24B and causing a deprotonation of the Nδ1 site or/and Asp25B residue. The next two steps are similar to those of the Lys171B exit pathway with overall 420 meV in stabilization energy. The two pathways have very similar energy profiles for proton ejection, with the Lys171B exit only slightly energetically more favorable and closer to the proton loading site, from which the pump proton is ejected.

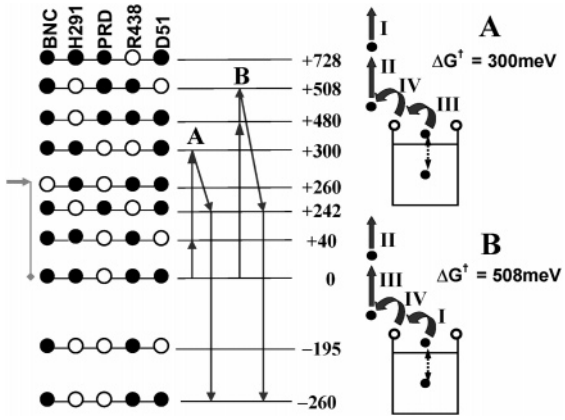

Figure 5. Asp51 proton exit pathway. The energy levels for the 10 lowest protonation states, which involve a proton in the BNC, His291, PRDa_3, Arg438, and Asp51, are shown. Depending on the sequence of the steps, a proton release via the Asp51 site may proceed by pushing a proton through a 300 meV (A) or 508 meV (B) high-energy barrier.

The proton connectivity between His291 and this site is not structurally as well defined as one to the Lys171B site. Contrary to Lys171B and Asp173B, His24B and Asp25B side chains are also not the conserved residues among cytochrome oxidases, and therefore, we consider this site less likely than Lys171B/Asp173B to be the proton release group.

Asp51 Exit Pathway. The second exit path from the Nδ1 site of His291 is via the PRD of heme a_3 that forms the salt bridge with Arg438, Figure 5. As in the path discussed above, here the key amino acids form a chain of protonatable sites, some are filled and some are empty, in which the protons can jump between the adjacent sites of the chain provided the acceptor site is empty. The energy profile depends on the sequence of proton transfer steps along the chain. Thus, we distinguished two possibilities, shown as parts A and B in Figure 5, with corresponding energy barriers of 300 and 508 meV. Interestingly, the sequence B that assumes a proton jump from His291 to PRDa_3 as the first step in the exit pathway is less favorable. The most favorable sequence of steps is one in which the deprotonation of Asp51 is the first step followed by an uphill (+260 meV) proton transfer from Arg438 to Asp51. The next two steps, proton jump from His291 to PRDa_3 and the reestablishment of the salt bridge, are downhill in energy by 60 and 500 meV, respectively.

The back-flow process, in which the loading site can receive a proton from the upper periplasmic side, is now even more disfavorable by at least 560 meV. Comparing the Asp51 proton exit pathway with the previous two, one can conclude that it is less favorable, or at least slower, since the energy barrier is higher. As for the specific barrier height, we have to note that in our calculations we used the X-ray structure of C*c*O in the fully oxidized form,[23] in which Asp51 is in its more buried conformation. As shown by Yoshikawa and co-workers, in the fully reduced form the side chain of Asp51 takes a more solvent exposed position, which would facilitate deprotonation of its carboxylic group. Exposing the Asp51 residue more to the solvent decreases its pK_a and lowers the energy barrier for the whole proton stroke process. In such circumstances the Asp51 proton exit pathway may have a somewhat lower barrier and become more competitive with the Lys171B and His24B/

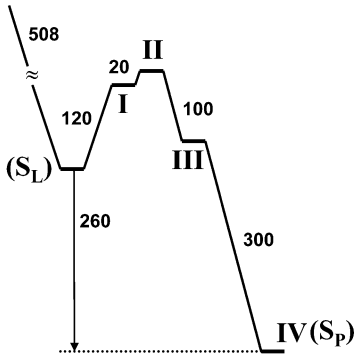

Figure 6. Energy diagram for the S_L to S_P transition. S_L is the metastable state with two repulsively interacting protons on the PLS and the BNC. S_P is the stable state which is formed after the pumping proton has been expelled from the enzyme.

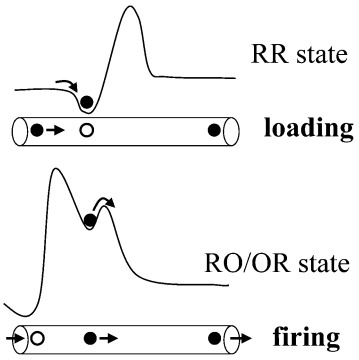

Figure 7. Schematic energy profiles for proton translocation along the membrane: (A) during the "loading" of the pumping site with the proton in the RR state; (B) during the "firing" of the loaded proton from the pumping site in the RO (or OR) state. The switch between the two profiles occurs upon entrance of the chemical proton to the BNC. The cycling between the two profiles makes the pump work.

Asp25B pathways (on the basis of our present calculations, however, the barrier cannot be lower than 260 meV; see Figure 5).

4. Discussion

On the basis of continuum electrostatic calculations described in this and the previous papers,[1,2] the following pumping mechanism in cytochrome oxidase is proposed. The proton loading site of the enzyme is the Nδ1 site of His291. This site is loaded upon electron transfer between the two hemes of the enzyme by a "fast" proton from Glu242.[48] Later, a "slower" second chemical proton is transferred to the binuclear center, via D- and possibly K-channels.[11−14,49−53] The Coulomb repulsion between the first pump proton and the second chemical proton results in the expulsion of the former from the Nδ1 site of His291 to the periplasmic side of the membrane. The working of the pump resembles that of a gun: in the loading step the PLS is loaded, while the transfer of the second proton causes the firing of the gun. The details of the loading stage, together with its energetics, are described in refs 1 and 2.

In this paper we described the energetics of the pumping stroke of C*c*O, and putative proton exit channels of the enzyme. The proton exit from the Nδ1 site of His291 is only possible via two propionates of heme a_3 (and an intermediate water molecule). Both PRAa_3 and PRDa_3 are hydrogen bonded and/or salt bridged, and the presence of an extra proton in these sites is energetically unfavorable. Therefore, to push a proton from His291 to the positive side of the membrane (upper side in all figures), a potential barrier must be overcome. We find that the exit channel via PRAa_3 is energetically more favorable, with a barrier of about 120 meV. This channel leads to two groups on the surface of the periplasmic side of the enzyme: Lys171B/Asp173B and His24B/Asp25B. The channel via PRDa_3 is less favorable, with a barrier higher than 260 meV, Figures 3 and 5. In both cases, the final steps of the proton exit along the exit channels are most energetically favorable, with a driving force greater than 400 meV. This characteristic of the exit channels is the key for blocking the back-flow of protons from the periplasmic side, because the first step in the back-transfer is the reversal of the last step of the exit transfer, and therefore has a barrier greater than 400 meV. The energetics of proton transfers along the most favorable exit channel PRAa_3 is shown in Figure 6, which summarizes results shown in Figures 4 and 5. The energy profile of the exit is practically the same for all four electrons and four protons pumped through the system. According to our model, ref 2, the loaded state of the pump, S_L in Figure 6, is metastable, and the stabilization occurs after the pumped proton is expelled from the His291 site. After each pumping event, a stable "pumped" state, S_P, is formed. The energy profile for the pumping stroke is shown in Figure 6.

The key feature of the proposed model is kinetic gating, which allows the pump to function without participation of the mechanical molecular gate (see also ref 54). The absence of significant structural movements in the crystal structures for different redox states is the key feature of cytochrome oxidase.[23] The kinetic gating is based on the specific energy profiles along the proton-conducting channel, which are qualitatively shown in Figure 7. These energy profiles were deduced from our electrostatic calculations.

In our model there are two stages of the pump cycle that occurs upon a passage of an electron through the enzyme, the loading and the firing, and the working of the pump resembles that of a gun. An electron transfer to the binuclear center occurs when one of the metal centers is formally oxidized (see the details in ref 2), and the proton loading site His291 is empty. Upon electron transfer between heme *a* and heme a_3, the proton loading site is protonated by a proton from the negative side of the membrane. This is the loading stage. It is essential that the PLS is loaded by a proton from the negative side of the membrane, and not from the opposite periplasmic side. The energy profile that results in this directionality is shown in Figure 7. The transfer from the periplasmic side is blocked by an energy barrier. When a chemical (slow) proton arrives at the BNC, the energy profile along the channel changes and assumes the form shown in the lower panel of Figure 7. The proton on His291, the PLS, becomes unstable, and is shifted from the PLS to the periplasmic side of the membrane. This is achieved by the specific energy profile shown in the figure. Thus, the key requirement for the pump that the pumped proton has to be taken from the negative side of the membrane and pushed to the opposite positive side is achieved by specific energy profiles in the loading and firing stages of the pump cycle shown in Figure 7. It is remarkable that electrostatic calculations that we have used to deduce the energetics of proton transfers result in such a consistent physical picture.

It should be noticed here that the protein is channeling protons against an external membrane potential (about 200 meV across the whole mitochondrial membrane). The obtained energy profiles (which do not include this additional membrane potential) show that there is more than enough energy available in the system for proton pumping against the membrane

potential. In physiological conditions, as a regulatory mechanism, the proton pumping, however, can be slowed or even impeded by increasing the membrane potential.[55]

The main proton exit channel leads from heme a_3 to Lys171B, which is buried in the interior of the enzyme but still is in contact with the external solvent. Looking from the outside, the protonated Lys171B is located at the bottom of the funnel formed by mostly hydrophobic residues. This enables the proton, released from Lys171B, to be rapidly expelled and delocalized in solvent and not retained in the vicinity of the release group. Also the access to the Lys171B site through the hydrophobic funnel, for a proton from the outside, is not very favorable and therefore most likely is not a very fast process. The results obtained from the electrostatic computations show that, besides the Lys171B exit channel, a proton pumping via two other proton release groups, His24B/Asp25B and Asp51 (and perhaps Asp300), might be energetically competitive under some circumstances, although the involvement is much less likely than that of Lys171B. In addition, we find that the protonation state of Asp173B is strongly coupled to that of Lys171B, and therefore, a pair of these residues can be considered as one exit site. A double mutation of these two residues would be interesting to examine.

In other cytochrome oxidases, for instance from *Rhodobacter Sphearoides*, Lys171B is substituted with an Arg, which can play the same role. Also adjacent Ile365 (located between Asp364 and Lys171B) in bovine C*c*O is replaced with Arg408 (*R. Sphearoides*) or Arg400 (*Paracoccus denitrificans*). Our test calculations show that Arg408 and Arg227B form the main proton exit pathway in *R. Sphearoides*, while the equivalent Arg400 and Lys191B become the main proton release groups in *P. denitrificans* C*c*O. It seems also that His117B (which occupies the position of bovine Lys171B) is potentially the best release group in ba_3-type cytochrome *c* oxidase from *Thermus thermophilus*. The results on the proton exit channels in other species will be reported elsewhere later.

The model discussed in this paper suggests an immediate experimental test of our predictions: one can modify one or several exit side chains shown in Figure 3 and thereby expect perturbation in the exit channel. Following the logic of the model, one should expect little change in the oxygen reduction turnover of the enzyme, but a change in the pumping activity of the enzyme. To predict results of such modifications in greater detail, additional calculations are needed. Such calculations are in progress in this group, and will be reported in our future publications.

Summarizing, we find that the most likely proton exit point on the periplasmic surface of cytochrome oxidase is Lys171B and possibly the coupled residue Asp173B. These two residues, compared with other potential exit sites, are most strongly coupled to His291, the loading site of the proposed pumping model.[1,2] It should be noticed that these two residues are conserved among the oxidases of different organisms. These two residues can be probed in the mutation experiments. According to our model, substitution of these residues to neutral residues should hinder or block the pumping, while preserving the reduction activity of the enzyme.

Acknowledgment. It is a pleasure to acknowledge stimulating discussions with Alexander Konstantinov of Moscow State University and Robert Gennis of the University of Illinois at Urbana-Champaign. This work has been supported by a research grant from the NIH (GM54052) and NSF.

References and Notes

(1) Popovic, D. M.; Stuchebrukhov, A. A. *J. Am. Chem. Soc.* **2004**, *126*, 1858.
(2) Popovic, D. M.; Stuchebrukhov, A. A. *FEBS Lett.* **2004**, *566*, 126.
(3) Wikström, M. *Curr. Opin. Struct. Biol.* **1998**, *8*, 480.
(4) Michel, H.; Behr, J.; Harrenga, A.; Kannt, A. *Annu. Rev. Biophys. Biomol. Struct.* **1998**, *27*, 329.
(5) Gennis, R. B. *Proc. Natl. Acad. Sci. U.S.A.* **1998**, *95*, 12747.
(6) Ferguson-Miller, S.; Babcock, G. T. *Chem. Rev.* **1996**, *7*, 2889.
(7) Wikström, M. *Biochemistry* **2000**, *39*, 3515.
(8) Michel, H. *Proc. Natl. Acad. Sci. U.S.A.* **1998**, *95*, 12819.
(9) Wikström, M. *Nature* **1989**, *338*, 776.
(10) Mitchell, P. *Nature* **1961**, *191*, 144.
(11) Konstantinov, A. A.; Siletsky, S.; Mitchell, D.; Kaulen, A.; Gennis, R. B. *Proc. Natl. Acad. Sci. U.S.A.* **1997**, *94*, 9085.
(12) Ädelroth, P.; Gennis, R. B.; Brzezinski, P. *Biochemistry* **1998**, *37*, 2470.
(13) Mills, D. A.; Ferguson-Miller, S. *Biochim. Biophys. Acta* **1998**, *1365*, 46.
(14) Brzezinski, P.; Ädelroth, P. *J. Bioenerg. Biomembr.* **1998**, *30*, 99.
(15) Mitchell, P.; Rich, P. R. *Biochim. Biophys. Acta* **1994**, *1186*, 19.
(16) Rich, P. R. *Aust. J. Plant Physiol.* **1995**, *22*, 479.
(17) Iwata, S.; Ostermeier, C.; Ludwig, B.; Michel, H. *Nature* **1995**, *376*, 660.
(18) Tsukihara, T.; Aoyama, H.; Yamashita, E.; Tomizaki, T.; Yamaguchi, H.; Shinzawa-Itoh, K.; Nakashima, R.; Yaono, R.; Yoshikawa, S. *Science* **1996**, *272*, 1136.
(19) Ostermeier, C.; Harrenga, A.; Ermler, U.; Michel, H. *Proc. Natl. Acad. Sci. U.S.A.* **1997**, *94*, 10547.
(20) Schmidt, B.; McCracken, J.; Ferguson-Miller, S. *Proc. Natl. Acad. Sci. U.S.A.* **2003**, *100*, 15539−15542.
(21) Wikström, M. *Biochim. Biophys. Acta* **2000**, *1458*, 188.
(22) Puustinen, A.; Wikstrom, M. *Proc. Natl. Acad. Sci. U.S.A.* **1999**, *96*, 35.
(23) Yoshikawa, S.; Shinzawa-Itoh, K.; Nakashima, R.; Yaono, R.; Yamashita, E.; Inoue, N.; Yao, M.; Fei, M. J.; Libeu, C. P.; Mizushima, T.; Yamaguchi, H.; Tomizaki, T.; Tsukihara, T. *Science* **1998**, *280*, 1723.
(24) Kawasaki, M.; Mogi, T.; Anraku, Y. *J. Biochem.* **1997**, *122*, 422.
(25) Pfitzner, U.; Odenwald, A.; Ostermann, T.; Weingard, L.; Ludwig, B.; Richter, O.-M. H. *J. Bioenerg. Biomembr.* **1998**, *30*, 89.
(26) Das, T. K.; Gomes, C. M.; Teixeira, M.; Rousseau, D. L. *Proc. Natl. Acad. Sci. U.S.A.* **1999**, *96*, 9591.
(27) Thomas, J. W.; Puustinen, A.; Alben, J. O.; Gennis, R. B.; Wikström, M. *Biochemistry* **1993**, *32*, 10923.
(28) Qian, J.; Shi, W.; Pressler, M.; Hogansson, C.; Mills, D.; Babcock, G. T.; Ferguson-Miller, S. *Biochemistry* **1997**, *36*, 2539.
(29) Popovic, D. M.; Quenneville, J.; Stuchebrukhov, A. A. *J. Phys. Chem. B*, to be published.
(30) Quenneville, J.; Popovic, D. M.; Stuchebrukhov, A. A. *J. Phys. Chem. B* **2004**, *108*, 18383.
(31) Onufriev, A.; Smondyrev, A.; Bashford, D. *J. Mol. Biol.* **2003**, *332*, 1183.
(32) Das, T. K.; Tomson, F. L.; Gennis, R. B.; Gordon, M.; Rousseau, D. L. *Biophys. J.* **2001**, *80*, 2039.
(33) Koutsoupakis, K.; Stavrakis, S.; Pinakoulaki, E.; Soulimane, T.; Varotsis, C. *J. Biol. Chem.* **2002**, *277*, 32860.
(34) Iwaki, M.; Rich, P. R. *J. Am. Chem. Soc.* **2004**, *126*, 2386.
(35) Spassov, V. Z.; Luecke, H.; Gerwert, K.; Bashford, D. *J. Mol. Biol.* **2001**, *312*, 203.
(36) Bashford, D.; Gerwert, K. *J. Mol. Biol.* **1992**, *224*, 473.
(37) Sampogna, R. V.; Honig, B. *Biophys. J.* **1994**, *66*, 1341.
(38) Bashford, D. An object-oriented programming suite for electrostatic effects in biological molecules. In *Scientific Computing in Object-Oriented Parallel Environments*; Ishikawa, Y., Oldehoeft, R. R., Reynders, J. V. W., Tholburn, M., Eds.; Springer: Berlin, 1997; Vol. 1343, p 233.
(39) Popovic, D. M.; Zaric, S. D.; Rabenstein, B.; Knapp, E. W. *J. Am. Chem. Soc.* **2001**, *123*, 6040.
(40) Popovic, D. M.; Zmiric, A.; Zaric, S. D.; Knapp, E. W. *J. Am. Chem. Soc.* **2002**, *124*, 3775.
(41) Rabenstein, B. Karlsberg online manual. http://lie.chemie.fu-berlin/karlsberg/ed, 1999.
(42) Lancaster, C. R.; Michel, H.; Honig, B.; Gunner, M. R. *Biophys. J.* **1996**, *70*, 2469.
(43) Kannt, A.; Lancaster, R. D.; Michel, H. *J. Bioenerg. Biomembr.* **1998**, *30*, 81.
(44) Kannt, A.; Lancaster, R. D.; Michel, H. *Biophys. J.* **1998**, *74*, 708.
(45) Okuno, D.; Iwase, T.; Shinzawa-Itoh, K.; Yoshikawa, S.; Kitagawa, T. *J. Am. Chem. Soc.* **2003**, *125*, 7209.
(46) Papa, S.; Capitanio, N.; Capitanio, G. *Biochim. Biophys. Acta* **2004**, *1655*, 353.

(47) Mills, D. A.; Florens, L.; Hiser, C.; Qian, J.; Ferguson-Miller, S. *Biochim. Biophys. Acta* **2000**, *1458*, 180.

(48) Zheng, X.; Medvedev, D. M.; Swanson, J.; Stuchebrukhov, A. A. *Biochim. Biophys. Acta* **2003**, *1557*, 99.

(49) Zaslavsky, D.; Gennis, R. B. *Biochim. Biophys. Acta* **2000**, *1458*, 164.

(50) Wikström, M.; Jasaitis, A.; Backgren, C.; Puustinen, A.; Verkhovsky, M. I. *Biochim. Biophys. Acta* **2000**, *1459*, 514.

(51) Hofacker, I.; Schulten, K. *Proteins* **1998**, *30*, 100.

(52) Karpefors, M.; Ädelroth, P.; Aagaard, A.; Sigurdson, H.; Svensson-Ek, M.; Brzezinski, P. *Biochim. Biophys. Acta* **1998**, *1365*, 159.

(53) Ruitenberg, M.; Kannt, A.; Bamberg, E.; Fendler, K.; Michel, H. *Nature* **2002**, *417*, 99.

(54) Stuchebrukhov, A. A. *J. Theor. Comput. Chem.* **2003**, *2*, 91.

(55) Kadenbach, B. *Biochim. Biophys. Acta* **2003**, *1604*, 77−94.